*Metrol. Meas. Syst.*, Vol. 26 (2019) No. 4, pp. 757–771
DOI: 10.24425/mms.2019.130565



PAN POLSKA AKADEMIA NAUK

METROLOGY AND MEASUREMENT SYSTEMS

Index 330930, ISSN 0860-8229
*www.metrology.pg.gda.pl*

M&MS

# A SAMPLING METHOD BASED ON IMPROVED FIREFLY ALGORITHM FOR PROFILE MEASUREMENT OF AVIATION ENGINE BLADE

**Zhi Huang, Liao Zhao, Kai Li, Hongyan Wang, Tao Zhou**

*University of Electronic Science and Technology of China, School of Mechanical and Electrical Engineering, 611731 Chengdu, China* (✉ *zhihuang@uestc.edu.cn*, +86 18 227 630 338, *zhaoliao_zl@163.com*, *457613088@qq.com*, *hongyanwang79@uestc.edu.cn*, *2914392726@qq.com*)

**Abstract**

Coordinate Measurement Machines (CMMs) have been extensively used in inspecting mechanical parts with higher accuracy. In order to enhance the efficiency and precision of the measurement of aviation engine blades, a sampling method of profile measurement of aviation engine blade based on the firefly algorithm is researched. Then, by comparing with the equal arc-length sampling algorithm (EAS) and the equi-parametric sampling algorithm (EPS) in one simulation, the proposed sampling algorithm shows its better sampling quality than the other two algorithms. Finally, the effectiveness of the algorithm is verified by an experimental example of blade profile. Both simulated and experimental results show that the method proposed in this paper can ensure the measurement accuracy by measuring a smaller number of points.

Keywords: aviation engine blade, coordinate measurement machine, profile measurement, improved firefly algorithm.



## 1. Introduction

Blades are the key and critical parts of the aviation engine, whose manufacturing precision impacts the aviation engine performance, efficiency and life limitation directly. In the development of high-performance aviation engine, higher requirements are placed on the manufacturing and inspection accuracy of the blades. Measurement accuracy requirements reach even a few microns, especially in the key areas such as the leading edge and trailing edge. Due to the complexity of the blade profile, the evaluation is generally achieved by measuring sectional curves distributed along the direction of the stacking line of the blade and comparing it with a blueprint (Fig. 1) [1]. Depending on the length and complexity of the blade, the number of sections required for measurement is also different. In general, the longer the blade and the more twisted the shape, the greater the number of sections needs to be measured. The standard template method is the traditional inspection of blade profile, but this inspection method involves highly skilled personnel due to using many templates. Moreover, this method's speed is inadequate. Currently, despite improvements of non-contact measurement methods, contact methods are still prevalent, especially when higher inspection accuracy is required. Therefore, the CMM has been the main tool for detecting blade contour manufacturing accuracy [2]. In theory, if numerous accurate points could be measured on a sectional curve, the geometric inspection would be performed very accurately. However, the scanning probe system, such as Renishaw REVO, is very expensive and cannot be widely used for blade measurement. Therefore, it is important to distribute measuring points correctly to improve the measurement efficiency of a CMM using contact probes.

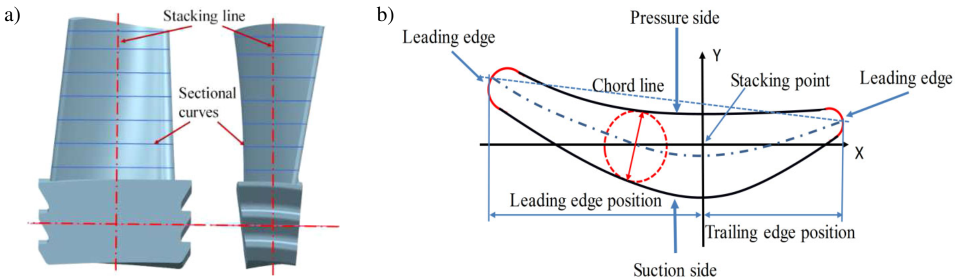


Fig. 1. The measurement cross-sections: a) the measurement sectional curves of blade; b) a blueprint of cross-sections.

Many researchers have devoted their effort to research sampling strategies on the free-form surface and have made progress [3]. A common method to generate the measurement sampling points on a free-form surface is the 2D grid method, which extracts the sampled data by projecting the external mesh nodes onto the surface. In this method, the number of sampling points is changed by adjusting the grid spacing, mainly including the Cartesian space uniform distribution method and the parameter space uniform distribution method [4]. However, this method is less adaptable to curved surfaces with complex curvature changes. Elkott *et al.* divided free-form surfaces into patches based on the knot vectors [5]. They distributed sampling points in these surface patches either based on patch size, mean Gaussian curvature of patch, or a combination of patch size and Gaussian curvature. Similarly, Obeidat and Raman considered three groups of points as critical points, which are the points with mean Gaussian curvatures, maximum Gaussian curvatures or average of the mean Gaussian curvature and minimum Gaussian curvature [6]. In addition, the chordal deviation method was presented, which can make the sampling points of a larger curvature area more densely distributed, and improve the accuracy of the sampling point fitting surface. But the drawback of this method is that it will cause the sampling point distribution in the region with small curvature to be too sparse, and reduce the overall fitting accuracy of the surface. To overcome this issue, Ainsworth et al. proposed a method of setting the minimum distance threshold of adjacent points based on the chordal deviation method, namely maximum chordal deviation [7].

Cho *et al.* proposed a method for obtaining curved sampling points by calculating the mean curvature [8]. In their methodology, the surface is subdivided into small regions specifically, and the regions are sorted according to the average curvature, and each region is adaptively sampled according to the region selection rate. Then, the points are more densely allocated on sub-sections with greater average curvature and less densely on sub-sections with smaller average curvature. Yu *et al.* presented an adaptive extraction method for free-surface CMM path sampling points based on the contour error model [9]. In their study, the accuracy of model contour restoration is effectively ensured by adopting the method of pre-existing boundary of the error model. However, the effect of the complex multi-surface is that the space's closed surface is wide, and the distribution points are too scattered, which affects the subsequent data processing efficiency. Poniatowska proposed a method that can increase the speed of inspection for similar parts [10]. In her method, the error distribution is obtained by uniform sampling and reconstructing the surface. Then, more points are distributed in areas with large errors. However, it needs many productions to build a reasonable model. Javad developed a new hybrid sampling strategy using *Particle Swarm Optimization* (PSO) method [11]. This method does not need the computations of geometric features such as curvature calculations or surface decomposition into smaller patches and all the sampling points are moved together with associated data in search to find their best positions. Since it is necessary to compare the deviation from the CAD model during each iteration, the efficiency needs to be improved.

Besides, a great deal of research on sampling strategies of blades has been done. Generally, a method to disperse points along a curve is either the equi-parametric or the equal arc-length one [5, 12]. However, with these methods it is difficult to obtain the key data in areas where the curvature of a curve changes sharply, such as the leading edge and the trailing edge of the blade. Subsequently, the solutions of this issue were presented by some researchers. Zhang *et al.* developed an adaptive discrete sampling algorithm based on the curvature of the blade sectional curves [13]. In their methodology, along the sectional curve, the spacing of each sampling point is determined according to the curvature at each point. However, this process is unidirectional and results in poor performance in the peripheral edge area. Huang *et al.* used a method of limiting the curvature distribution range of the maximum and minimum curvature positions on the parametric curve to determine the weight proportion of each parameter position, so that to adjust the pre-discrete sampling points according to the equal arc-length method [14]. Although the problem of uneven sampling in the outlying edge region is solved, the intermediate portion of the curve may appear at the intersection position during the iteration. Additionally, Mansour *et al.* proposed a precise process to extract the minimum set of measurement points, using the method of 3rd degree polynomial to achieve a better fitted accuracy [15]. However, this method was used for simulating objects by three-dimensional scanning and the number of initial sampling points was considerable. Jiang *et al.* presented a method for extracting the sampling points of the leading edge curve and trailing edge curve of the blade section according to the chordal deviation criterion [16]. The sampling density was limited by specifying the maximum chordal deviation and each section was also sampled considering the chordal deviation difference threshold.

In sum, the blade sectional curve is complex. The curvature of the leading and trailing edges differs greatly from the curvature of the leaf back. Some blind sampling strategies, such as equal arc-length sampling, need excessive number of measurement points, which is time-consuming. Other adaptive sampling strategies, such as chordal deviation criterion, can easily cause the sampling points to be excessively distributed in the leading edge and trailing edge areas with large curvature. According to the previous studies, areas with large mean curvature are considered to be the areas with a great probability of leading to large machining errors [17]. So it is a very effective method to select sampling points based on curvature. Just like Javad proposed, it has not only to place more points in places with large deviations, but also needs to find the best placement of these points [11]. The key issue is how to distribute the sampling points over different curvature regions. In the firefly algorithm, each firefly determines the flight direction and the adaptive motion step size depending on the brightness of adjacent fireflies, and repeatedly updates the position of each firefly to achieve the purpose of optimizing the position distribution of the population. Similarly to this principle, the sampling points find their best positions in the sectional curves according to curvature attraction. In this research, the firefly algorithm has been used to search for the best positions of sampling points across blade sectional curves.

## 2. Blade surface curve representation

The CAD model of an aviation engine blade is typically generated by a set of 2D-blade sectional curves along the stacking axis [18], which can be expressed by an NURBS surface as follows:

$$S(u,v) = [x(u,v),\ y(u,v),\ z(u,v)]^T = \frac{\sum_{i=0}^{n}\sum_{j=0}^{m} w_{i,j} P_{i,j} N_{i,p}(u) N_{i,q}(v)}{\sum_{i=0}^{n}\sum_{j=0}^{m} w_{i,j} N_{i,p}(u) N_{i,q}(v)} \qquad 0 \le u,\quad v \le 1, \tag{1}$$

where: $P_{i,j}$ are control points; $w_{i,j}$ are weights; $N_{i,p}(u)$ are B-spline basis functions over $u$ and $N_{i,q}(v)$ are B-spline basis functions over $v$.

Usually, the sectional curves are obtained by establishing a spatial plane and intersecting with the CAD model of blade, which can be expressed:

$$C(u) = \frac{\sum_{i=0}^{n} w_i p_i N_{i,k}(u)}{\sum_{i=0}^{n} w_i N_{i,k}(u)}, \tag{2}$$

where: $p_i$ are control points; $w_i$ are weights and $N_{i,k}(u)$ are B-spline basis functions over $u$. $N_{i,k}(u)$ is expressed:

$$\begin{cases} N_{i,0}(u) = \begin{cases} 1 & u_i < u < u_{i+1} \\ 0 & \text{else} \end{cases} \\ N_{i,k}(u) = \dfrac{(u-u_i)N_{i,k-1}(u)}{u_{i+k}-u_i} + \dfrac{(u_{i+k+1}-u)N_{i+1,k-1}(u)}{u_{i+k+1}-u_{i+1}} \end{cases}. \tag{3}$$

## 3. Developed measurement sampling strategy

### *3.1. Segmentation of sectional curves*

When sampling the overall sectional curves, there is generally a problem of uneven sampling. A way to solve this problem is to divide the sectional curves into different regions roughly according to the curvature. As shown in Fig. 2, a sectional curve is divided into four parts: $P_1$, $P_2$, $P_3$ and $P_4$, referring to the areas of leading edge part, trailing edge part, suction side and pressure side of the blade, respectively. The detailed steps are as follows.

Firstly, calculate the total length $D$ of the sectional curve:

$$\begin{aligned} D &= \sum_{j=0}^{n-1} \int_{u_j}^{u_{j+1}} \sqrt{[c_x'(u)]^2 + [c_y'(u)]^2 + [c_z'(u)]^2}\, du \\ &= \int_0^1 \sqrt{[c_x'(u)]^2 + [c_y'(u)]^2 + [c_z'(u)]^2} du, \end{aligned} \tag{4}$$

where $c_x'(u)$, $c_y'(u)$, $c_z'(u)$ are differentials of the arc.

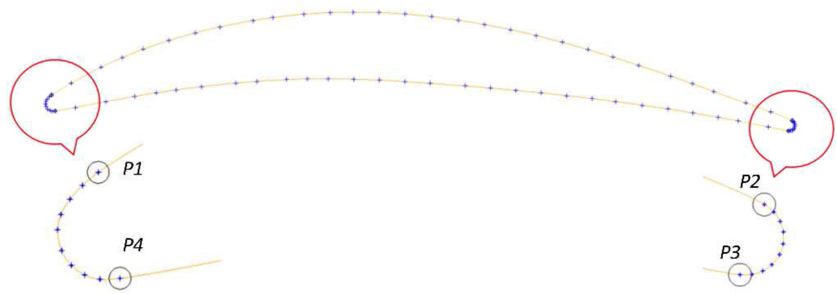


Fig. 2. A schematic diagram of blade sectional curves' segmentations.

Secondly, define the number of sampling points $N$ and calculate the unit arc length $d$:

$$d = \frac{D}{N}\,. \tag{5}$$

Thirdly, substitute $d$ into (6) to obtain the calculation parameters at each point:

$$d = \int\limits_{u_j}^{u_{j+1}} \sqrt{\left[c_x'(u)\right]^2 + \left[c_y'(u)\right]^2 + \left[c_z'(u)\right]^2} du. \tag{6}$$

Then, draw a circle with the current position as the centre and $d$ as the radius. Obtain the intersection of the circle and the section curve in the direction of the parameter. In order to improve the accuracy of dispersing sectional curves, the arc length is subdivided into smaller segments, and the unit arc length is replaced by the sum of these segments. Based on these points, the centroid point $(x_0, y_0)$ is roughly calculated. Find two points $j_1$ and $j_2$ with the largest distance from the centroid point when $x > 0$ and $x < 0$, respectively. Take the point $j$ around $j_1$ and $j_2$ respectively, and fit the circle by the least square method.

$$Q_j(a,b,c) = \min\left[\sum_{i=1}^{n}\left(x_i^2 + y_i^2 + ax_i + by_i + c\right)^2\right]. \tag{7}$$

Finally, select the circle with the highest fitting accuracy according to the different values of $j$. Extract the first and last two points of the intersection of the circle and the sectional curve as the segmentation points $P_1$, $P_2$, $P_3$ and $P_4$.

$$P(x,y,z) = \min[Q_j(a,b,c)]. \tag{8}$$

### *3.2. Improved Firefly Algorithm (IFAS) of extracting sampling points*

The firefly algorithm was proposed by Yang [14] in 2008 and is suitable for addressing the problem of optimal path and multi-point optimization. In the algorithm, all fireflies are unisex so that one firefly will be attracted to other fireflies regardless of their sex. Attractiveness is proportional to the brightness, which decreases with increasing distance between fireflies. If there are no brighter fireflies than a particular firefly, this individual will move randomly in the space. The main steps are as follows:

1. The brightness of each firefly can be approximated using the following Gaussian form:

$$I(r) = I_0 \, e^{-\beta r^2}, \tag{9}$$

where $I_0$ is the initial brightness when $r = 0$, $\beta$ represents a light absorption coefficient ($\beta \in [0, +\infty)$), which in the actual application generally takes $\beta \in [0.1, \ldots, 10]$, and $r$ is the distance between two fireflies.

2. Calculate the attractiveness $\gamma_{i,j}(r)$ between two fireflies:

$$\gamma_{i,j}(r_{i,j}) = \gamma_0 \, e^{-\beta r_{i,j}^2}, \tag{10}$$

where $\gamma_0$ is the attractiveness at $r_{i,j} = 0$, usually taken as 1 in practical engineering applications. The distance between any two fireflies $i$ and $j$ at $X_i(t)$ and $X_j(t)$ can be defined as the Cartesian distance:

$$r_{i,j} = \|X_j(t) - X_i(t)\|. \tag{11}$$

Here, $r_{i,j}$ is the distance between two fireflies and $t$ is the number of iterations. $X_i(t)$ indicates the current position of the current firefly.

3. Update the location during iteration:

$$X_i(t+1) = X_i(t) + \gamma_{i,j}(r_{i,j}) \left[X_j(t) - X_i(t)\right] + \alpha \varepsilon_i\,, \tag{12}$$

where $\alpha$ is a randomization parameter, generally taken as $\alpha \in [0, 1]$, and subject to the standard normal distribution. $\varepsilon_i$ is a random vector either obeying the Gaussian distribution or evenly distributed.

Based on the firefly algorithm, the moving direction of a sampling point and the adaptive moving step are determined by comparing the light intensity between three points on the sectional curves. The curvatures of the leading/trailing edge areas and the suction/pressure areas differ greatly. In order to prevent excessive concentration of sampling points, set a threshold $\varepsilon$ between two adjacent sampling points. The adaptive distribution of sampling points on the curve is obtained by continuously updating the sampling point positions. A flowchart of the algorithm is shown in Fig. 3.

A detailed description of the above-mentioned process follows.

Step 1. Set a threshold $\varepsilon$, the maximum number of iterations $T$ and the number of sampling points $n$ in each area. Distribute the sampling points on the sectional curves uniformly with the equal arc-length sampling method.

Step 2. Extract successively 3 adjacent points $(i, j, k)$ from these discrete sampling points to constitute a small firefly community. According to the calculation formula of curvature:

$$\kappa = \left|C'(u_i) \times C''(u_i)\right| \Big/ \left|C'(u_i)\right|^3 \tag{13}$$

calculate the curvature $(\kappa_i, \kappa_j, \kappa_k)$ in each position of the 3 points and the arc length $(L_{ij}, L_{jk})$ between adjacent points, respectively. Then, calculate the brightness of the point $i$ to point $j$ and point $k$ to point $j$, $I_{ij}^{(i)} = \kappa_i \, e^{-\beta^{L_{ij}^2}}$, $I_{jk}^{(k)} = \kappa_k \, e^{-\beta^{L_{jk}^2}}$. Next, calculate the brightness of point $j$ to point $i$ and point $j$ to point $k$: $I_{ij}^{(j)} = \kappa_j \, e^{-\beta^{L_{ij}^2}}$, $I_{jk}^{(j)} = \kappa_j \, e^{-\beta^{L_{jk}^2}}$. Finally, by comparing $I_{ij}^{(i)}$, $I_{ij}^{(j)}$, $I_{jk}^{(k)}$ and $I_{jk}^{(j)}$ respectively, the moving direction of the middle point (point $j$) is determined.

Step 3. If point $j$ moves toward point $i$, calculate the arc length $L_{ij}$ between point $i$ and $j$. Then, substitute $L_{ij}$ into formula (10) to calculate the attractiveness $\gamma_{ij}$. Similarly, if point $j$ moves toward point $k$, calculate the arc length $L_{jk}$ and the attractiveness $\gamma_{jk}$. The position of point $j$ is updated according to (12), and the moving step size is determined by (12). According to the actual sampling demand, the moving step size can be appropriately reduced by (14) to improve the sampling accuracy, as follows:

$$X_i(t+1) = X_i(t) + \frac{\gamma_{i,j}(r_{i,j})[X_j(t) - X_i(t)]}{2} + \frac{\theta^t \varepsilon_i}{2}, \tag{14}$$

where $\theta$ is a randomization parameter, taken [0.9, 0.95] according to different blades. $t$ is the number of iterations.

Step 4. Suppose that point $j$ moves to point $k$. Take the coordinate of point $j$ as the centre and the step size of the move from point $j$ to $k$ as the radius to draw a circle. The circle intersects the sectional curves at point $j'(X_j'(t+1))$. Calculate the arc length $l_j(t+1)$ between points $j'$ and $k$. Then, compare $l_j(t+1)$ with the threshold $\varepsilon$. If $l_j(t+1) \geq \varepsilon$, then point $j$ moves to $j'$. Similarly, after all the positions of these sampling points have been updated, calculate the sum of the distances of all sampling points $L$ and compare it with the original arc length $D$.

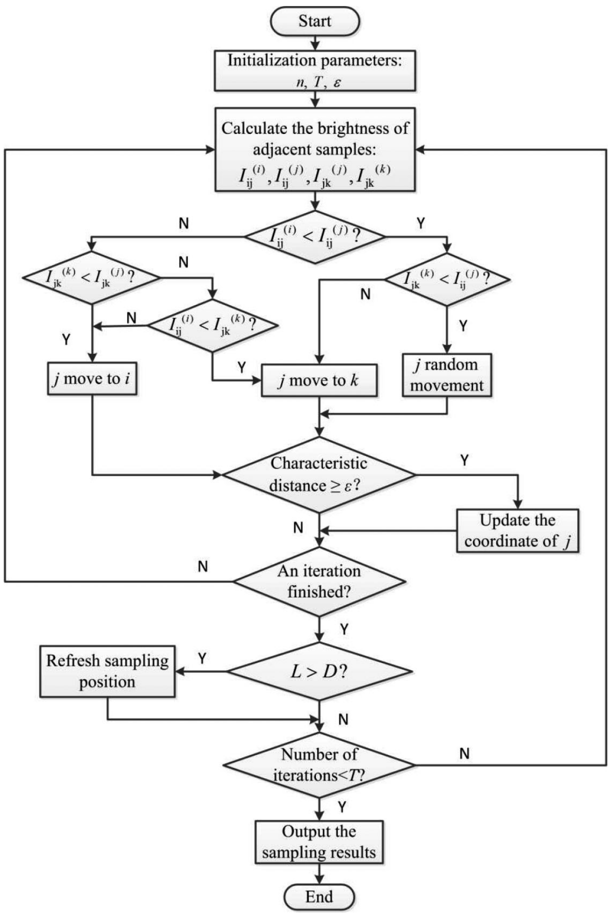


Fig. 3. A flowchart of the algorithm.

Finally, extract the corresponding sampling points when $L$ is closest to $D$ in the iterative process.

In sum, in order to adapt to the characteristics of blade measurement, and to prevent the firefly algorithm from falling into a local optimum, the improvement of the firefly algorithm is mainly reflected in the following.

1. Set a corresponding threshold $\varepsilon$ to prevent excessive concentration of sampling points.
2. Gradually narrow the search step size by parameters $\theta$ and $t$ to increase search accuracy.

## 4. Demonstrations and discussion

### *4.1. Experimental studies*

In this section there will be demonstrated some examples and analysis. The sampling results obtained by the proposed strategy are shown in Fig. 4. It can be observed that the approach employed in this study can ensure the sampling density at high curvature portion. For each sectional curve, there are 10 sampling points on the leading edge and trailing edge respectively, and 30 sampling points on the suction/pressure surfaces. In this blade, the maximum distance of two adjacent sampling points is about 5.34 mm. The locations of four segment points, which are obtained by the above mentioned method, is obviously marked.

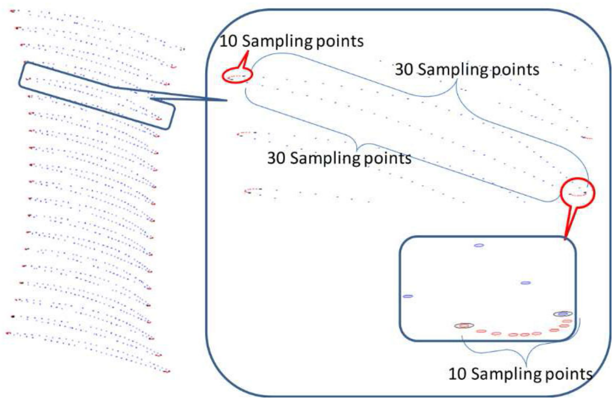


Fig. 4. A schematic diagram of sampling points' distribution.

In order to verify the precision of the algorithm proposed in this study, different algorithms were compared. First, the sectional curve was sampled by using equal arc-length sampling, equi-parametric sampling and improved firefly algorithm sampling methods, respectively. Then, three sampling point sets were fitted to a B-spline curve. The differences between the original curve and the curves fitted by data of 80 points from each reduction method is shown in Fig. 5. From the comparison and analysis, it can be seen that the algorithm of this paper exhibits a better fitting accuracy than the other two methods in the leading edge and trailing edge parts. Then, the advantages of this algorithm are demonstrated by comparing with the other two methods in contour deviation, maximum position deviation and average position deviation. As shown in Fig. 6, all sectional curves, fitted with 40, 80, 120 and 160 measuring points, are analysed and compared. The contour deviation of blade section indicates the difference between the distance sum of adjacent sampling points and the total length of the sectional curve. The smaller the difference, the higher the fitting accuracy of the sampling point curve. The position deviation of

Metrol. Meas. Syst., Vol. 26 (2019), No. 4, pp. 757–771
DOI: 10.24425/mms.2019.130565

the blade profile (shown in Fig. 7), which is obtained by discretely fitting the curve and calculating the distance from each discrete point to the actual contour curve, indicates the biggest difference between the sampling point fitting curve and the actual sectional curve of the blade section. Fig. 8 shows the comparison of average position deviation of sectional curves of the blade.

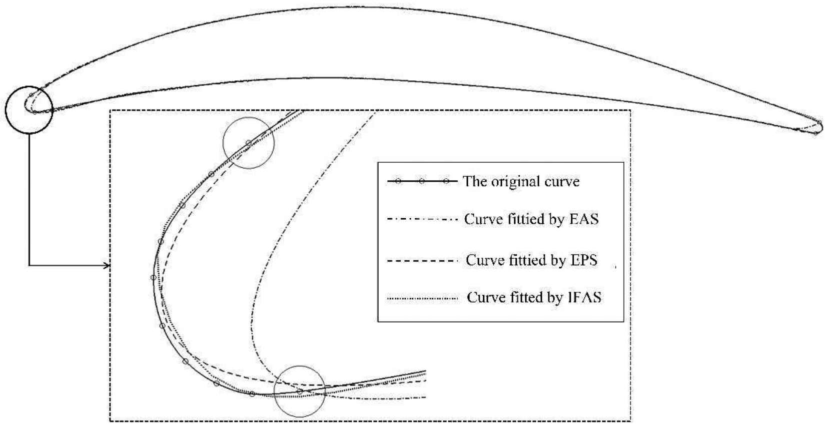


Fig. 5. A schematic diagram of fitting curves obtained with different sampling algorithms for sectional curves of the blade.

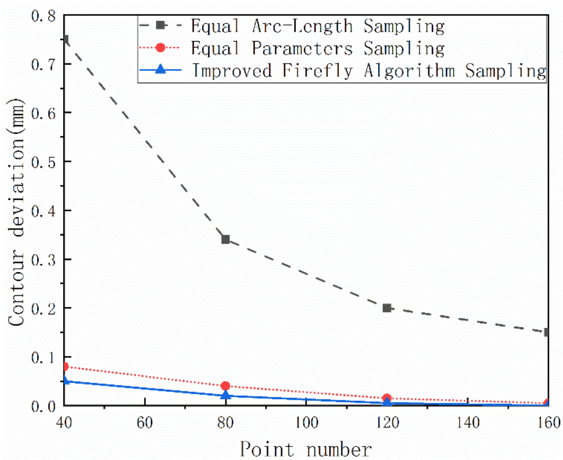


Fig. 6. Comparison of contour deviation of sectional curves.

It can be observed in these figures that the fitting accuracy of the proposed algorithm is superior to those of the other two algorithms in both the blade profile deviation and the position deviation. Especially in the leading edge and trailing edge parts, the curve fitted by the algorithm of this paper fits best with the original CAD model. Moreover, as the number of sampling points decreased, the fitting error greatly increased in the other two methods. The method proposed in this paper can fit the blade sectional curve well for fewer sampling points. For this blade, the algorithm of this paper only needs about half the number of sampling points of the other two algorithms to achieve the same sampling accuracy, which proves the effectiveness and superiority of the proposed strategy.

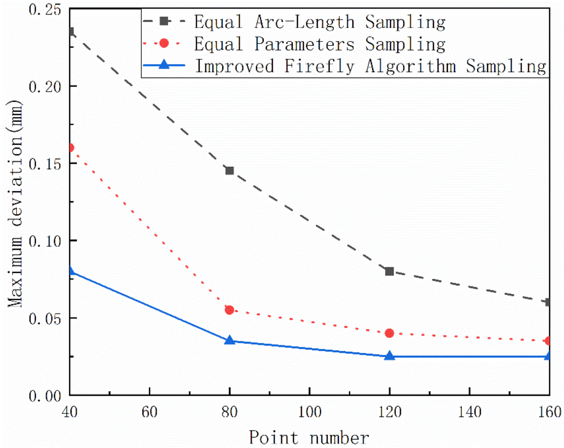


Fig. 7. Comparison of maximum position deviation of sectional curves.

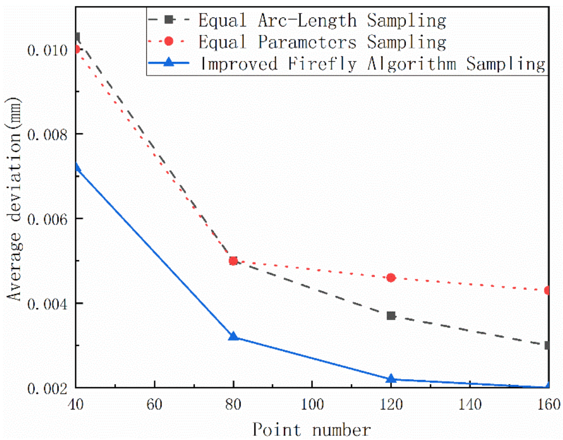


Fig. 8. Comparison of average position deviation of sectional curves.

In order to verify the reliability of this algorithm, the blade was measured using a CMM of HEXAGON. The measured sectional curves and the blade are shown in Fig. 9. The difference is that the number of sampling points for the equal arc-length and the equi-parametric methods is 120, whereas for the proposed algorithm it is 80. In this experiment, the measurement was performed three times for each sampling strategy to check data consistency. Then, the deviation from the obtained substitute geometry and CAD models was computed by using the commercial software Geomagic. Fig. 10 shows the error maps obtained with equal arc-length sampling, equi-parametric sampling and the developed sampling strategies, respectively. It can be seen that the area with the largest deviation is on the leading edge and the trailing edge, especially for the equal arc-length and equi-parametric sampling. The IFAS can fit the leading edge and trailing edge curves well. The maximum deviation and error area obtained with IFAS are smaller than those obtained with the other two sampling methods. In addition, compared with the other two sampling methods, the alternative geometry of using IFAS fits better to the CAD model of the

DOI: 10.24425/mms.2019.130565

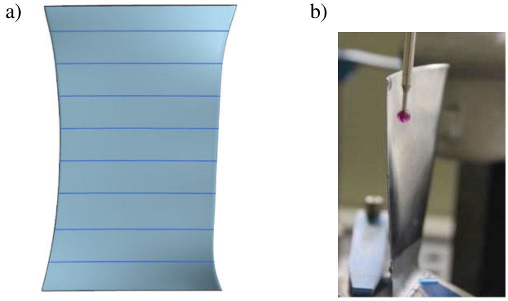


Fig. 9. The measurement experiment: a) the measured sectional curves; b) CMM for blade measurement.

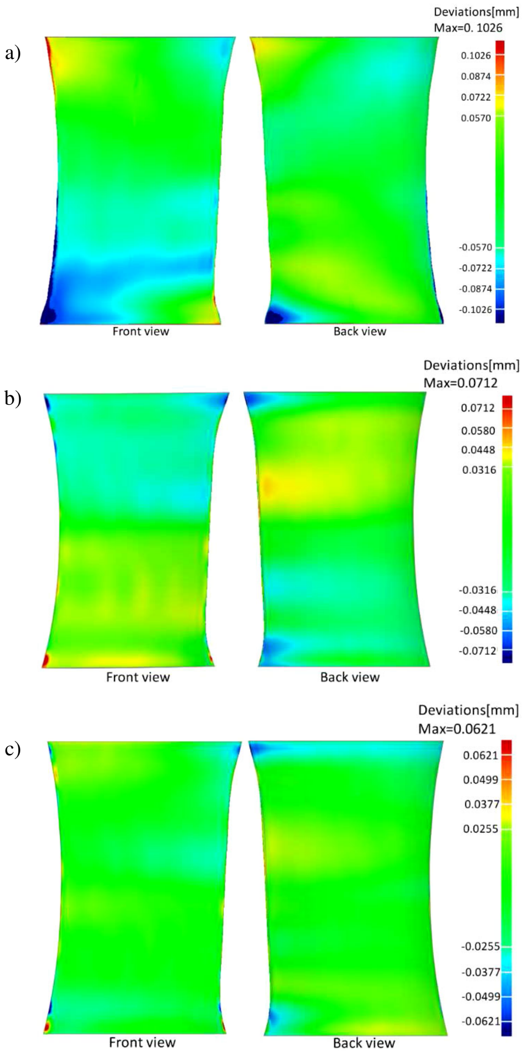


Fig. 10. Substitute geometry deviation from the CAD model obtained with different sampling strategies, a) EAS; b) EPS; c) IFAS.

blade. As we can see from Fig. 10, the upper and lower edges of the blade have large errors, which results from the fact that the shape of the blade is twisted and bent greatly in these two regions and needs more measured sectional curves.

Since the small number of measurement points are sampled, the substitute geometry and the CAD model might have larger deviations locally, such as the area between two sectional curves. The Geomagic software was used to compare the maximum deviation and average deviation of reconstructed substitute curves obtained with the CAD model from the sectional curves. The absolute values of the deviations is given in Table 1. Clearly, the method proposed in this study can reduce the number of sampling points, still ensuring accuracy.

Table 1. Comparison results of EAS, EPS and IFAS.

| **Sampling method** | **Measurement points on each curve** | **Maximum deviation (mm)** | **Average deviation (mm)** |
|---|---|---|---|
| Equal arc-length | 120 | 0.082 | 0.005 |
| Equi-parametric | 120 | 0.051 | 0.004 |
| Improved firefly algorithm | 80 | 0.038 | 0.002 |

Furthermore, the proposed method was compared with another two more advanced and effective sampling strategies, namely the *chordal deviation* (CDS) and *particle swarm optimization sampling* (PSO) by simulations [11]. The simulations were performed on a computer (Core i5 CPU 2.5 GHz, RAM 8 GB). Fig. 11 shows the distributions of 60 sampling points across the sectional curve for different strategies, respectively. Obviously, all strategies can guarantee more sampling points on the leading edge and the trailing edge. The proposed strategy can ensure that there are enough sampling points on the pressure side and suction side of the blade. Fig. 12 shows the deviations of the fitted curves from the original CAD curve. It can be seen that the coincidence between the fitting curves obtained with the three strategies and the CAD curve is very high. Since using PSO distributes more points on the leading edge and the trailing edge regions, the deviation from the CAD model is smaller in these areas than that obtained with IFAS. Although using the CDS has good fitting accuracy in leading/ trailing edge regions, the fitting accuracy is greatly reduced in the pressure/suction sides because the numbers of sampling points are too small. As we can see, the proposed method can ensure better sampling accuracy in

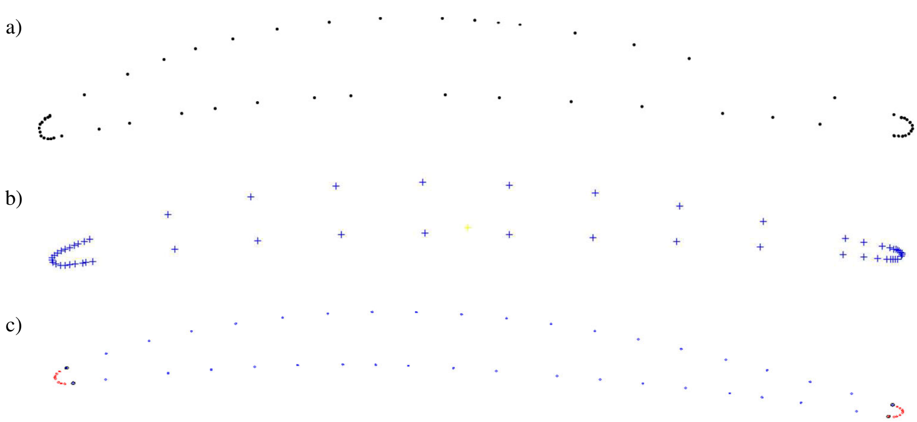


Fig. 11. Distributions of sampling points: a) using CDS; b) using PSO; c) using IFAS.

Metrol. Meas. Syst., Vol. 26 (2019), No. 4, pp. 757–771
DOI: 10.24425/mms.2019.130565

suction and pressure sides than the other two methods. In addition, the calculation time of PSO is longer than CDS and IFAS, and the latter two are similar. The comparison results of the two measurement strategies are shown in Table 2.

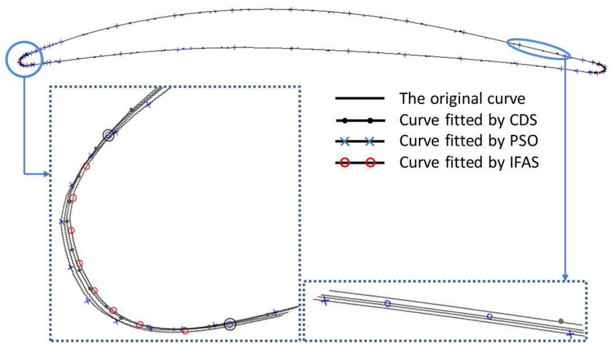


Fig. 12. Deviations of the fitted curves from the original CAD curve.

Table 2. Comparison results of CDS, PSO and IFAS.

| | Number of measurement points | Maximum deviation (mm) | Average deviation (mm) | Time (sec) |
|---|---|---|---|---|
| CDS | 60 | 0.095 | 0.011 | 35 |
| PSO | 60 | 0.048 | 0.005 | 69 |
| IFAS | 60 | 0.056 | 0.005 | 42 |

### *4.2. Discussion*

The major advantages of the developed method are that it can reconstruct the sectional curve precisely with fewer measurement points. In other words, the proposed method can reduce the number of points that is required for measuring the blades using CMM and reduce the test time. The reasons are as follows:

1. According to the feature of the blade, the sectional curve was divided into four sections and the sampling points were distributed over every section by using the equal arc-length sampling strategy. Then, the sampling points were moved to find the best positions by judging the curvature and distance between two adjacent points. Each point moved only locally to find the best position. The moving target of each point is clear and the calculation is simple. The calculation time of this method is greater than that of the equal arc-length and equi-parametric methods, but it saves a great deal of measurement time.
2. For the other adaptive sampling algorithms, such as the chordal deviation, only position of the next measurement point can be decided, because the rest of measurement points are previously allocated to fixed positions [11]. In the proposed method, similarly to the PSO algorithm, every point will be moved to find the best position. The difference is that each particle in PSO needs to consider three factors in each iteration, namely the current position of the particle, the best position for this particle through previous searches, and the best position within the whole of particle population, to determine the moving direction. And the PSO algorithm needs to reconstruct the substitute geometry and obtain the deviation from the CAD model. Although the accuracy is increased, it costs much computation time.

## 5. Conclusions and scope of future work

To practically implement the blade measurement, a sampling method based on the improved firefly algorithm has been proposed. In this sampling strategy, the sectional curve is divided into four sections according to the blade characteristic and the equal arc-length algorithm is used to distribute the sampling points along the sectional curves. Then, the improved firefly algorithm is employed to identify the best positions of measurement sample points. By comparing with two traditional sampling methods, the experimental results show that the proposed method saves inspection time and increases accuracy of sampling strategy. At last, compared with the particle swarm algorithm, the advancement of the method is demonstrated.

Based on the proposed sampling strategy, we have developed a blade data analysis software (shown as Fig. 13) with independent intellectual property rights, which greatly reduces the difficulty of data matching and pre-processing, improves and facilitates the quality level of the blade evaluation. It lays a technical foundation for subsequent blade reconstruction and adaptive processing.

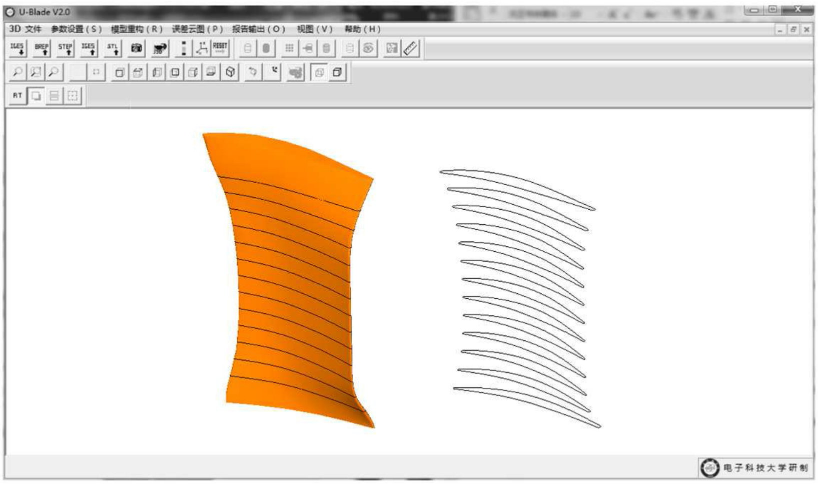


Fig. 13. Blade surface data analysis software.

The technique can be improved and applied to the free-form surface sampling. The research is underway.

## Acknowledgements

The authors gratefully acknowledge the support of the National Natural Science Foundation of China (Nos. 51275078).

### References

[1] Hoschek, J., Müller, R. (2000). Turbine blade design by lofted B-spline surfaces. *Journal of Computational & Applied Mathematics*, 119(1–2), 235–248.

[2] Zhi, H., Chao, L., Kai, L. (2017). Status and prospect of detection technology of coordinate measuring machine for blade surface of aero-engine. *Aeronautical Manufacturing Technology*, 21, 73–79.

[3] Fiona, Z., Xun, X., Xie, S.Q. (2009). Computer-Aided inspection planning – The state of the art. *Computer in Industry*, 60(7), 453–466.

[4] Rajamohan G., Shunmugam, M., Samuel, G. (2011). Practical measurement strategies for verification of freeform surfaces using coordinate measuring machines. *Metrol. Meas. Syst.*, 18(2), 209–222.

[5] Elkott, D.F., Elmaraghy, H.A., Elmaraghy, W.H. (2002). Automatic sampling for CMM inspection planning of free-form surfaces. *International Journal of Production Research*, 40(11), 2653–2676.

[6] Obeidat, S.M., Raman, S. (2009). An intelligent sampling method for inspecting free-form surfaces. *International Journal of Advanced Manufacturing Technology*, 40(11–12), 1125–1136.

[7] Ainsworth, I., Ristic, M., Brujic, D. (2000). CAD-based measurement and path planning for free-form shapes using contact probes. *International Journal of Advanced Manufacturing Technology*, 16(1), 23–31.

[8] Cho, M.W., Kim, K. (1995). New inspection planning strategy for sculptured surfaces using coordinate measuring machine. *International Journal of Production Research*, 33(2), 427–444.

[9] Ming, R.Y., Ying, J.Z., Li, Y.L., Zhang, D. (2013). Adaptive sampling method for inspection planning on CMM for free-form surfaces. *International Journal of Advanced Manufacturing Technology*, 67(9–12), 1967–1975.

[10] Poniatowska, M. (2012). Deviation model based method of planning accuracy inspection of free-form surfaces using CMMs. *Measurement*, 45(5), 927–937.

[11] Javad, Z., Hossein, A., Vahid, M. (2018). A hybrid measurement sampling method for accurate inspection of geometric errors on freeform surfaces. *Measurement*, 122, 155–167.

[12] Rajamohan, G., Shunmugam, M.S., Samuel, G.L. (2011). Effect of probe size and measurement strategies on assessment of freeform profile deviations using coordinate measuring machine. *Measurement*, 44(5), 832–841.

[13] Dong, X.Z., Kun, B., Yong, Y.C. (2012). Research on CMM-based measuring points' sampling and distribution method of blades. *Forging & Stamping Technology*, 37(4), 137–141.

[14] Yun, G.H., Xin, H., Kui, W.M., Cun, Y.S., Min, G.Y. (2016). CAD-based measurement planning strategy of complex surface for five axes on machine verification. *International Journal of Advanced Manufacturing Technology*, 91(5), 1–11.

[15] Mansour, G. (2014). A developed algorithm for simulation of blades to reduce the measurement points and time on coordinate measuring machine. *Measurement*, 54, 51–57.

[16] Song, R.J., Wen, H.W., Hua, D.Z., Qiang, Z.Q. (2014). A practical sampling method for profile measurement of complex blades. *Measurement*, 81, 57–65.

[17] He, G., Sang, Y., Pang, K., Sun, G. (2018). An improved adaptive sampling strategy for freeform surface inspection on cmm. *International Journal of Advanced Manufacturing Technology*, 96(2), 1521–1535.

[18] Xinshe, Y. (2010). Nature-inspired metaheuristic algorithms. *Luniver Press*.